Continuous-variable entanglement of phase-locked light beams

H. H. Adamyan[1,2,*] and G. Yu. Kryuchkyan[1,2,†]

[1]*Yerevan State University, A. Manookyan 1, 375049, Yerevan, Armenia*

[2]*Institute for Physical Research, National Academy of Sciences, Ashtarak-2, 378410, Armenia*

(Received 3 September 2003; revised manuscript received 30 January 2004; published 18 May 2004)

We explore in detail the possibility of intracavity generation of continuous-variable (CV) entangled states of light beams under mode phase-locked conditions. We show that such quantum states can be generated in a self-phase-locked nondegenerate optical parametric oscillator (NOPO) based on type II phase-matched down-conversion combined with a linear mixer of two orthogonally polarized modes of the subharmonics in a cavity. A quantum theory of this device, recently realized in the experiment, is developed for both subthreshold and above-threshold operational regimes. We show that the system providing high-level phase coherence between two generated modes, unlike the ordinary NOPO, also exhibits different types of quantum correlations between photon numbers and phases of these modes. We quantify the CV entanglement as two-mode squeezing and show that the maximal degree of the integral two-mode squeezing (which is 50% relative to the level of vacuum fluctuations) is achieved at the pump field intensity close to the generation threshold of a self-phase-locked NOPO, provided that the constant of linear coupling between the two polarizations is much less than the mode detunings. The peculiarities of CV entanglement for the case of unitary, nondissipative dynamics of the system under consideration are also cleared up.

I. INTRODUCTION

It is now believed that entanglement of quantum composite systems with a continuous degree of freedom is the basis of most applications in the field of quantum information [1]. Interest in continuous-variable (CV) entanglement is being extensively excited by successful experiments on quantum teleportation based on two-mode squeezed states [2] as well as the experiments dealing with entanglement in atomic ensembles [3]. Since then, remarkable theoretical and experimental efforts have been devoted to generating and quantifying CV entangled states.

In this paper we propose a type of CV entangled states of light-field with reduced phase noise. They are different from the well-known entangled Einstein-Podolsky-Rosen (EPR) states generated in a nondegenerate optical amplifier [4,5], which exhibit large phase fluctuations. We believe that such entangled states of light-field with localized phases can be generated in a self-phase-locked nondegenerate optical parametric oscillator (NOPO), based on the type II phase-matched down-conversion and additional phase-locking process stipulated by the intracavity waveplate. The motivations for this study are the following.

The CV entangled states of light were studied in [4] and demonstrated experimentally in [5] for a nondegenerate optical parametric amplifier (NOPA). Then a CV entanglement source was built from two single-mode squeezed vacuum states combined on a beam splitter [2]. It is well known that each of the orthogonally polarized and frequency degenerate fields generated by NOPO is a field of zero-mean values. The phase sum of generated modes is fixed by the phase of the pump laser, while their phase difference undergoes a phase diffusion process [4] stipulated by vacuum fluctuations. As a rule, the NOPO phase diffusion noise is substantially greater than the shot noise level, which limits the usage of NOPO in precision phase-sensitive measurements. Various methods based on phase-locking mechanisms [6–10] have been proposed for reducing such phase diffusion. In the comparatively simple scheme realized in the experiment [6], self-phase-locking was achieved in NOPO by adding an intracavity quarter-wave plate to provide polarization mixing between two orthogonally polarized modes of the subharmonics. The evidence of self-phase-locking was provided there by the high level of phase coherence between the signal and idler fields. Following this experiment, the semiclassical theory of such NOPO was developed in [7]. Recently, schemes of multiphoton parametric oscillators based on cascaded down-conversion processes in $\chi^{(2)}$ media placed inside the same cavity and showing self-phase-locking have been proposed [8]. As was demonstrated in [9], the system based on a combination of OPO and second-harmonic generation also displays self-phase-locking. The formation of self-phase-locking and its connection with squeezing in the parametric four-wave mixing under two laser fields has been demonstrated in [10]. An important characteristic of self-phase-locked devices concerns the phase structure of generated subharmonics. Indeed, the formation of the variety of distinct phase states under self-phase-locked conditions has been obtained in Refs. [6–10]. It was recently noted that the schemes involving phase locking are potentially useful for precise interferometric measurements and optical frequency division because they combine fine-tuning capability and stability of type II phase matching with effective suppression of phase noise. That is why we believe it will be interesting to consider phase-locked dynamics also from the perspective of quantum optics and, in particular, from the standpoint of production of CV entanglement.

A further motivation for such a task is connected with the problem of experimental generation of bright entangled light.

*Email address: adam@unicad.am

†Email address: gkryuchk@server.physdep.r.am
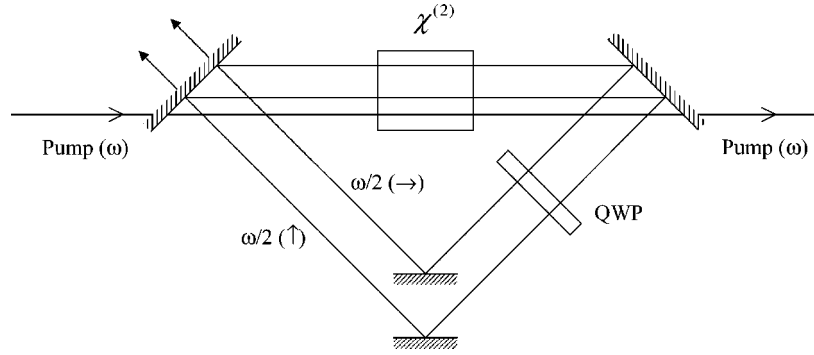
FIG. 1. The principal scheme of a self-phase-locked NOPO in a triply resonant cavity for the pump mode at frequency ω and two subharmonic modes of two orthogonal polarizations ($\uparrow$) and ($\rightarrow$) at frequency $\omega/2$. We have chosen the special path for the pump mode to underscore the fact that the pump mode rapidly decays ($\gamma_3 \gg \gamma_1, \gamma_2$) and is eliminated adiabatically. The type II phase-matching condition for the process $\omega \rightarrow \omega/2(\uparrow) + \omega/2(\rightarrow)$ is satisfied in the $\chi^{(2)}$ medium. The intracavity quarter waveplate (QWP) provides a polarization mixing between the orthogonally polarized subharmonics.

So far, to the best of our knowledge, there has been no experimental demonstration of CV entanglement above the threshold of NOPO. Progress in experimental study of a bright two-mode entangled state from a cw nondegenerate optical parametric amplifier has been made in [11]. A theoretical investigation of CV entangled light in transition through the generation threshold of NOPO is given in [12]. One of the principal experimental difficulties in attaining a high-intensity level is the impossibility to control the frequency degeneration of modes above the threshold. We hope that the usage of phase-locked NOPO may open a new interesting possibility to avoid this difficulty.

In this paper, we report what is believed to be the first investigation of self-phase-locked CV entangled states. We develop the quantum theory of self-phase-locked NOPO, with decoherence included, in application to the generation of such entangled states. This scheme is based on a combination of two processes, namely type II parametric down-conversion and linear polarization mixing with cavity-induced feedback. The parametric down-conversion is a standard technique used to produce entangled photon pairs as well as CV two-mode squeezed states [2]. The beam splitter and the polarization mixer are also considered to be experimentally accessible devices for production of entangled light-fields [13]. Besides these, there have been some studies of a beam splitter for various nonclassical input states, including two-mode squeezing states [14]. It is obvious, and also follows from the results of [8–10], that the operational regimes of the combined system with cavity-induced feedback and dissipation drastically differ from those for pure processes. We show below that an analogous situation takes place in the investigation of quantum-statistical properties of a combined system such as the self-phase-locked NOPO.

The paper is arranged as follows. In Sec. II we formulate the model of the combined NOPO based on the processes of two-photon splitting and polarization mixing, and we present a semiclassical analysis of the system. Section III is devoted to an analysis of quantum fluctuations of both modes within the framework of the linearization procedure around the stable steady state. In Sec. IV we investigate the CV entangling resources of self-phase-locked NOPO on the basis of

two-mode squeezing for both subthreshold and above-threshold operational regimes. We also discuss in Sec. IV the case of unitary, nondissipative dynamics using a well-justified small-interaction-time approximation. We summarize our results in Sec. V.

II. MODEL OF SELF-PHASE-LOCKED NOPO

As an entangler we consider a combination of two processes in a triply resonant cavity, namely type II parametric down-conversion in a $\chi^{(2)}$ medium and polarization mixing between subharmonics in a lossless symmetric quarter-wave plate. The Hamiltonian describing intracavity interactions is

$$H = i\hbar E(e^{i(\Phi_L - \omega t)}a_3^+ - e^{-i(\Phi_L - \omega t)}a_3) + i\hbar k(e^{i\Phi_k}a_3 a_1^+ a_2^+ - e^{-i\Phi_k}a_3^+ a_1 a_2) + \hbar\chi(e^{i\Phi_\chi}a_1^+ a_2 + e^{-i\Phi_\chi}a_1 a_2^+), \tag{1}$$

where a_i are the boson operators for the cavity modes ω_i. The mode a_3 at frequency ω is driven by an external field with amplitude E and phase Φ_L, while a_1 and a_2 describe subharmonics of two orthogonal polarizations at degenerate frequencies $\omega/2$. The constant $ke^{i\Phi_k}$ determines the efficiency of the down-conversion process. The linear coupling constant denoted as $\chi e^{i\Phi_\chi}$ describes the energy exchange between only the subharmonic modes, χ is determined by the amount of polarization rotation due to the intracavity waveplate, and Φ_χ determines the phase difference between the transformed modes. We take into account the detunings of subharmonics Δ_i and the cavity damping rates γ_i and consider the case of high cavity losses for pump mode ($\gamma_3 \gg \gamma_1, \gamma_2$), when this mode can be adiabatically eliminated. However, in our analysis we take into account the pump depletion effects. The principal scheme of this device, the so-called self-phase-locked NOPO, is shown in Fig. 1 for the special configuration when the coupling of in- and out-radiation fields occurs at one of the ring cavity mirrors. Note that a comparison of this configuration with the analogous one considered in [7], where the pump field is a traveling wave, is discussed below.

Due to the explicit presence of dissipation in this problem, one has to write the master equation for the reduced density

matrix of the system. The reduced density operator ρ within the framework of the rotating wave approximation and in the interaction picture is governed by the master equation

$$\frac{\partial \rho}{\partial t} = \frac{1}{i\hbar}[H',\rho] + \sum_{i=1}^{3} \gamma_i(2a_i\rho a_i^+ - a_i^+ a_i\rho - \rho a_i^+ a_i), \quad (2)$$

where

$$H' = \sum_{i=1}^{3} \hbar\Delta_i a_i^+ a_i + i\hbar E(a_3^+ - a_3) + i\hbar k(a_3 a_1^+ a_2^+ - a_3^+ a_1 a_2)$$
$$+ \hbar\chi(a_1^+ a_2 + a_1 a_2^+). \quad (3)$$

Let us also note that this equation is rewritten through the transformed boson operators $a_i \rightarrow a_i \exp(-i\Phi_i)$, with Φ_i being $\Phi_3 = \Phi_L$, $\Phi_2 = \frac{1}{2}(\Phi_L + \Phi_k - \Phi_\chi)$, $\Phi_1 = \frac{1}{2}(\Phi_L + \Phi_k + \Phi_\chi)$. That leads to a cancellation of the phases on the intermediate stages of calculations. As a result, the Hamiltonian H' depends only on real-valued coupling constants.

In order to proceed further, we now consider the phase-space symmetry properties of the two subharmonic modes. It is easy to check that the interaction Hamiltonian satisfies the commutation relation $[H', U(\pi)]=0$ with the operator $U(\theta) = \exp[i\theta(a_1^+ a_1 - a_2^+ a_2)]$. Moreover, analogous symmetry $[\rho(t), U(\pi)]=0$ takes place for the density operator of the system, which obeys the master equation (2). Using this symmetry we establish the following selection rules for the normal-ordered moments of the mode operators of the subharmonics:

$$\langle a_1^{+k} a_2^{+m} a_1^l a_2^n \rangle = 0, \quad (4)$$

if $k+l+m+n \neq 2j$, $j=0, \pm 1, \pm 2, \ldots$. Another peculiarity of NOPO with Hamiltonian (1) is displayed in the phase space of each of the subharmonic modes. The reduced density operator for each of the modes is constructed from the density operator ρ by tracing over the other modes $\rho_1 = \text{Tr}_2\text{Tr}_3(\rho)$, $\rho_2 = \text{Tr}_1\text{Tr}_3(\rho)$. Therefore, we find that $[\rho_1(t), U_1(\pi)] = [\rho_2(t), U_2(\pi)]=0$, where $U_i(\theta) = \exp(i\theta a_i^+ a_i)$ $(i=1,2)$ is the rotation operator. It is easy to check using these equations that the Wigner functions W_1 and W_2 of the modes have a twofold symmetry under the rotation of the phase space by angle π around its origin,

$$W_i(r,\theta) = W_i(r, \theta + \pi), \quad (5)$$

where r, θ are the polar coordinates of the complex phase space. Note that such symmetry relationships (4) and (5) radically differ from those taking place for the usual NOPO without the quarter-wave plate. Indeed, in this case [the case of $\chi=0$ in Eqs. (1)–(3)], the Wigner functions W_i are rotationally symmetric and the symmetry properties (4) read as $\langle a_1^{+k} a_1^l a_2^{+m} a_2^n \rangle = 0$ if $k-l \neq m-n$.

We perform concrete calculations in the positive P representation [15] in the frame of stochastic equations for the complex c-number variables α_i and β_i corresponding to the operators a_i and a_i^+,

$$\frac{\partial \alpha_1}{\partial t} = -(\gamma_1 + i\Delta_1)\alpha_1 + k\alpha_3\beta_2 - i\chi\alpha_2 + R_1, \quad (6)$$

$$\frac{\partial \beta_1}{\partial t} = -(\gamma_1 - i\Delta_1)\beta_1 + k\beta_3\alpha_2 + i\chi\beta_2 + R_1^+, \quad (7)$$

$$\frac{\partial \alpha_3}{\partial t} = -\gamma_3\alpha_3 + E - k\alpha_1\alpha_2, \quad (8)$$

$$\frac{\partial \beta_3}{\partial t} = -\gamma_3\beta_3 + E - k\beta_1\beta_2. \quad (9)$$

The equations for α_2, β_2 are obtained from Eqs. (6) and (7) by exchanging the subscripts $(1) \rightleftarrows (2)$. $R_{1,2}$ are Gaussian noise terms with zero means and the following nonzero correlators:

$$\langle R_1(t)R_2(t') \rangle = k\alpha_3\delta(t - t'), \quad (10)$$

$$\langle R_1^+(t)R_2^+(t') \rangle = k\beta_3\delta(t - t'). \quad (11)$$

Recall that we consider the regime of adiabatic elimination of the pump mode. In this approach, the stochastic amplitudes α_3 and β_3 are given by

$$\alpha_3 = (E - k\alpha_1\alpha_2)/\gamma_3, \quad (12)$$

$$\beta_3 = (E - k\beta_1\beta_2)/\gamma_3. \quad (13)$$

Substituting amplitudes α_3, β_3 into Eqs. (6), (7), (10), and (11), we arrive at

$$\frac{\partial \alpha_1}{\partial t} = -(\gamma_1 + i\Delta_1)\alpha_1 + (\varepsilon - \lambda\alpha_1\alpha_2)\beta_2 - i\chi\alpha_2 + R_1, \quad (14)$$

$$\frac{\partial \beta_1}{\partial t} = -(\gamma_1 - i\Delta_1)\beta_1 + (\varepsilon - \lambda\beta_1\beta_2)\alpha_2 + i\chi\beta_2 + R_1^+, \quad (15)$$

$$\langle R_1(t)R_2(t') \rangle = (\varepsilon - \lambda\alpha_1\alpha_2)\delta(t - t'), \quad (16)$$

$$\langle R_1^+(t)R_2^+(t') \rangle = (\varepsilon - \lambda\beta_1\beta_2)\delta(t - t'). \quad (17)$$

Here $\varepsilon = kE/\gamma_3$, $\lambda = k^2/\gamma_3$. So Eqs. (14) and (15) and corresponding equations for α_2, β_2, involve the depletion effect of the pump mode, which leads to the appearance of the above-threshold operational regime.

It should be noted that Eqs. (8) and (9) for the pump mode amplitude do not involve terms of the linear coupling between the modes of subharmonics. From this we can immediately recognize that Eqs. (12) and (13) and hence Eqs. (14) and (15) take place for arbitrary values of the parameter χ. Nevertheless, the effect of linear coupling between the modes is displayed in the dynamics of the pump mode through the amplitudes α_1 and α_2. In the adiabatic approach, these effects are described through the pump depletion terms $k\alpha_1\alpha_2/\gamma_3$, $k\beta_1\beta_2/\gamma_3$ in the expressions for the pump field amplitudes (12) and (13) and hence are completely taken into consideration in Eqs. (14) and (15) as well as in the correlators (16) and (17).

First, we shall study the steady-state solution of the sto-chastic equations in semiclassical treatment, ignoring the noise terms for the mean photon numbers n_{j0} and phases φ_{j0} of the modes $[n_j = \alpha_j \beta_j, \varphi_j = (1/2i)\ln(\alpha_j/\beta_j)]$. The mean pho-ton numbers read

$$n_{10}^{\pm} = \frac{1}{\lambda}\left(\frac{\Delta_2}{\Delta_1}\right)^{1/2}[\sqrt{\varepsilon^2 - (\varepsilon_{cr}^{\pm})^2 + \widetilde{\gamma}^2} - \widetilde{\gamma}], \qquad (18)$$

$$n_{20}^{\pm} = \frac{1}{\lambda}\left(\frac{\Delta_1}{\Delta_2}\right)^{1/2}[\sqrt{\varepsilon^2 - (\varepsilon_{cr}^{\pm})^2 + \widetilde{\gamma}^2} - \widetilde{\gamma}], \qquad (19)$$

where

$$\widetilde{\gamma} = \frac{\gamma_1}{2}\left(\frac{\Delta_2}{\Delta_1}\right)^{1/2} + \frac{\gamma_2}{2}\left(\frac{\Delta_1}{\Delta_2}\right)^{1/2}. \qquad (20)$$

As we can see from Eqs. (18) and (19), $n_{10}^{\pm}$ and $n_{20}^{\pm}$ are real and positive for ε exceeding two critical points,

$$(\varepsilon_{cr}^{\pm})^2 = \gamma_1\gamma_2 + \Delta_1\Delta_2 + \chi^2 \mp \sqrt{4\chi^2\Delta_1\Delta_2 - (\gamma_1\Delta_2 - \gamma_2\Delta_1)^2}, \qquad (21)$$

and, besides, the solutions n_{i0}^{+} and n_{i0}^{-} ($i=1,2$) correspond to two distinct values ε_{cr}^{+} and ε_{cr}^{-} accordingly. The steady-state values of the phases corresponding to each of the critical points ε_{cr}^{-}, ε_{cr}^{+} are obtained as

$$\sin(\varphi_{20}^{+} - \varphi_{10}^{+}) = \sin(\varphi_{20}^{-} - \varphi_{10}^{-})$$
$$= \frac{1}{2\chi}\left[\gamma_1\left(\frac{\Delta_2}{\Delta_1}\right)^{1/2} - \gamma_2\left(\frac{\Delta_1}{\Delta_2}\right)^{1/2}\right], \quad (22)$$

$$\cos(\varphi_{20}^{\pm} + \varphi_{10}^{\pm}) = \frac{1}{\varepsilon}\sqrt{\varepsilon^2 - (\varepsilon_{cr}^{\pm})^2 + \widetilde{\gamma}^2}. \qquad (23)$$

It is easy to check that these solutions exist for both modes only if the following relation holds:

$$4\chi^2\Delta_1\Delta_2 > (\gamma_1\Delta_2 - \gamma_2\Delta_1)^2. \qquad (24)$$

Let us note that the steady-state solutions (22) and (23) com-pletely determine the absolute phases of the orthogonally polarized modes, which are hence self-locked, unlike the or-dinary NOPO. These results are in accordance with the ones obtained in [6,7], but for another configuration of NOPO. In the scheme proposed in [6], only the signal and idler modes are excited in the cavity, while the pump field is a traveling wave. Nevertheless, in the adiabatic regime considered here there is correspondence between both schemes. Indeed, it is not difficult to check that the results (18) and (19) transform to the corresponding results of the mentioned scheme [7] by replacing the parameter ε with the corresponding pump field amplitude.

We now turn to the standard linear stability analysis of these solutions, assuming for simplicity perfect symmetry between the modes, provided that the cavity decay rates and the detunings do not depend on the polarization ($\gamma_1 = \gamma_2 = \gamma, \Delta_1 = \Delta_2 = \Delta$). The stability of the system is governed by the matrices F and F_+, F_- describing the dynamics of small deviations $\delta\alpha_i$ and $\delta\beta_i$ from the semiclassical steady-state

solutions (see. Sec. III). We reach stability if the real parts of eigenvalues of these matrices are positive. This analysis dis-plays an evident dependence on the sign of the detunings $\Delta_1 = \Delta_2 = \Delta$. For the positive detuning, $\Delta > 0$, only the steady-state solutions $n_{10}^{-} = n_{20}^{-}$ and $\varphi_{20}^{-} - \varphi_{10}^{-}$, $\varphi_{20}^{-} + \varphi_{10}^{-}$ are stable, while for the case of negative detuning the stability holds for the solutions with the $(+)$ superscript. As this analysis shows, for either sign of detuning, the threshold is reached at $\varepsilon \geq \varepsilon_{th}$, where

$$\varepsilon_{th} = \sqrt{(\chi - |\Delta|)^2 + \gamma^2}, \qquad (25)$$

and the steady-state stable solution for mean photon numbers can be written in the general form as

$$n_0 = n_{10} = n_{20} = \frac{1}{\lambda}[\sqrt{\varepsilon^2 - (\chi - |\Delta|)^2} - \gamma]. \qquad (26)$$

The phases are found to be

$$\varphi_{10} = \varphi_{20} = -\frac{1}{2}\arcsin\frac{1}{\varepsilon}(\chi + |\Delta|) + \pi k \qquad (27)$$

for $\Delta > 0$. For the opposite sign of the detuning, $\Delta < 0$, as we noted, the mean photon numbers are given by the same Eq. (26), while the phases read

$$\varphi_{10} = \frac{1}{2}\arcsin\frac{1}{\varepsilon}(\chi + |\Delta|) + \pi\left(k + \frac{1}{2}\right),$$

$$\varphi_{20} = \frac{1}{2}\arcsin\frac{1}{\varepsilon}(\chi + |\Delta|) + \pi\left(k - \frac{1}{2}\right) \qquad (28)$$

($k=0,1,2,\ldots$). In the region $\varepsilon \leq \varepsilon_{th}$, the stability condition is fulfilled only for the zero-amplitude steady-state solution $\alpha_1 = \alpha_2 = \beta_1 = \beta_2 = 0$. So, the set of above-threshold stable so-lutions for both modes has twofold symmetry in phase space, which was indeed expected from symmetry arguments (5).

Let us now consider the output behavior of the system for the special scheme of generation, when the couplings of in and out fields occur at only one of the ring-cavity mirrors (see Fig. 1). Taking into account that only the fundamental mode is coherently driven by the external field with $\langle\alpha_3^{in}\rangle = E/\gamma_3$, while the subharmonic modes are initially in the vacuum state, we obtain for the mean photon numbers (in units of photon number per unit time) $n_3^{in} = E^2/2\gamma_3, n_i^{out} = 2\gamma_i n_{i0}(i=1,2)$ and hence $n_1^{out} = n_2^{out} = 2\gamma n_0$. Accordingly, parametric oscillation can occur above the threshold pump power $P_{th} = \hbar\omega^3 E_{th}^2/2\gamma_3$, where the threshold value of the pump field is equal to

$$E_{th} = \frac{\gamma_3}{k}\sqrt{(\chi - |\Delta|)^2 + \gamma^2}. \qquad (29)$$

We are now in a position to study quantum effects in self-phase-locked NOPO and will state the main results of the paper concerning CV entanglement.

III. ANALYSIS OF QUANTUM FLUCTUATIONS

The aim of the present section is to study the quantum-statistical properties of self-phase-locked NOPO in linear

treatment of quantum fluctuations. Quantum analysis of the system using the P representation is standard. A detailed description of the method can be found in [15]. We assume that the quantum fluctuations are sufficiently small so that Eqs. (14) and (15) can be linearized around the stable semiclassical steady state $\alpha_i(t) = \alpha_i^0 + \delta\alpha_i(t)$, $\beta_i(t) = \beta_i^0 + \delta\beta_i(t)$. This is appropriate for analyzing the quantum-statistical effects, namely CV entanglement, for all operational regimes with the exception of the vicinity of threshold, where the level of quantum noise increases substantially. It should also be emphasized at this stage that in the above-threshold regime of a self-phase-locked NOPO, the steady-state phases of each of the modes are well-defined in contrast to what happens in the case of ordinary NOPO, where phase diffusion takes place. According to this effect, the difference between the phases, as well as each of the phases, cannot be defined in the above-threshold regime of generation of the ordinary NOPO. On the whole, the well-founded linearization procedure cannot be applied for this case. Nevertheless, the linearization procedure and analysis of quantum fluctuations for ordinary NOPO become possible due to the additional assumptions about temporal behavior of the difference between the phases of the generated modes [16].

We begin with a consideration of the below-threshold operational regime, for $E < E_{\text{th}}$, where the equations linearized around the zero-amplitude solution can be written in the following matrix form:

$$\frac{\partial}{\partial t}\delta\alpha^\mu = -F_{\mu\nu}\delta\alpha^\nu + R^\mu(\alpha,t), \qquad (30)$$

where $\mu = 1,2,3,4$ and $\delta\alpha^\mu = (\delta\alpha_1, \delta\alpha_2, \delta\alpha_3, \delta\alpha_4) = (\delta\alpha_1, \delta\alpha_2, \delta\beta_1, \delta\beta_2)$, $R^\mu = (R_1, R_2, R_1^+, R_2^+)$. The 4×4 matrix $F_{\mu\nu}$ is written in the block form

$$F = \begin{pmatrix} A, & B \\ B^*, & A^* \end{pmatrix} \qquad (31)$$

with 2×2 matrices

$$A = \begin{pmatrix} \gamma + i\delta, & i\chi \\ i\chi, & \gamma + i\delta \end{pmatrix}, \quad B = \varepsilon\begin{pmatrix} 0, & 1 \\ 1, & 0 \end{pmatrix}. \qquad (32)$$

The noise correlators are determined as

$$\langle R^\mu(\alpha,t)R^\nu(\alpha,t')\rangle = D_{\mu\nu}(\alpha)\delta(t-t') \qquad (33)$$

with the following diffusion matrix:

$$D = \begin{pmatrix} B, & 0 \\ 0, & B^* \end{pmatrix}. \qquad (34)$$

First, we calculate the temporal correlation functions of the fluctuation operators. The expectation values of interest can be written as the integral

$$\langle\delta\alpha^\mu(t)\delta\alpha^\nu(t')\rangle = \int_{-\infty}^{\min(t,t')} d\tau (e^{F(t-\tau)}De^{F^T(t'-\tau)})_{\mu\nu}, \quad (35)$$

F^T being the transposition of the matrix F. The integration over $d\tau$ can be performed using the following useful formula for operators $DF^T = FD$, obtained by straightforward calcula-

tion. As a consequence, we arrive at the expression $De^{F^T t} = e^{Ft}D$. Finally we obtain

$$\langle\delta\alpha^\mu(t)\delta\alpha^\nu(t')\rangle = -\frac{1}{2}(F^{-1}e^{F|t-t'|}D)_{\mu\nu}, \qquad (36)$$

and hence for $t = t'$

$$\langle\delta\alpha^\mu(t)\delta\alpha^\nu(t)\rangle = -\frac{1}{2}(F^{-1}D)_{\mu\nu}. \qquad (37)$$

This formula, however, is not very convenient for practical calculations. Therefore, we rewrite the correlation functions of the quantum fluctuations $\delta\alpha_i, \delta\beta_i$ in a more simple form through the two-dimensional column vectors $\delta\alpha = (\delta\alpha_1, \delta\alpha_2)^T$, $\delta\beta = (\delta\beta_1, \delta\beta_2)^T$. Upon performing the calculation, we finally arrive at

$$\langle\delta\alpha(\delta\alpha)^T\rangle = \frac{\varepsilon}{S^4 - 4\Delta^2\chi^2}\left[\gamma\begin{pmatrix} -2\chi\Delta, & S^2 \\ S^2, & -2\chi\Delta \end{pmatrix} \right.$$
$$\left. -i\begin{pmatrix} \chi(S^2 - 2\Delta^2), & \Delta(S^2 - 2\chi^2) \\ \Delta(S^2 - 2\chi^2), & \chi(S^2 - 2\Delta^2) \end{pmatrix}\right],$$

$$\langle\delta\alpha(\delta\beta)^T\rangle = \frac{\varepsilon^2}{2(S^4 - 4\Delta^2\chi^2)}\begin{pmatrix} S^2, & -2\chi\Delta \\ -2\chi\Delta, & S^2 \end{pmatrix}, \quad (38)$$

where S^2 is introduced as

$$S^2 = \gamma^2 + \chi^2 + \Delta^2 - \varepsilon^2. \qquad (39)$$

Note that $S^2 > 0$ in the below-threshold regime.

As an application of these results, the mean photon number in the below-threshold regime can be calculated as follows:

$$n_1 = n_2 = \frac{\varepsilon^2 S^2}{2(S^4 - 4\Delta^2\chi^2)}. \qquad (40)$$

Next we focus on the mode-locked regime, for $E > E_{\text{th}}$, considering Eqs. (14) and (15) in terms of the fluctuations $\delta n_i(t) = n_i(t) - n_{i0}$ and $\delta\varphi_i(t) = \varphi_i(t) - \varphi_{i0}$ of photon number and phase variables. In this regime, the dynamics described by the linearized equations of motion actually decouples into two independent dynamics for two groups of combinations $\delta n_\pm = \delta n_2 \pm \delta n_1$, $\delta\varphi_\pm = \delta\varphi_2 \pm \delta\varphi_1$. In fact, one has

$$\frac{\partial}{\partial t}\begin{pmatrix} \delta n_+ \\ \delta\varphi_+ \end{pmatrix} = -F_+\begin{pmatrix} \delta n_+ \\ \delta\varphi_+ \end{pmatrix} + \begin{pmatrix} R_{n+} \\ R_{\varphi+} \end{pmatrix}, \qquad (41)$$

$$\frac{\partial}{\partial t}\begin{pmatrix} \delta n_- \\ \delta\varphi_- \end{pmatrix} = -F_-\begin{pmatrix} \delta n_- \\ \delta\varphi_- \end{pmatrix} + \begin{pmatrix} R_{n-} \\ R_{\varphi-} \end{pmatrix}. \qquad (42)$$

The drift, $F_\pm$, and the diffusion matrices, $\langle R_i(t)R_j(t')\rangle = D_{ij}^{(+)}\delta(t-t')$ $(i,j = n_+, \delta\varphi_+)$, $\langle R_n(t)R_m(t')\rangle = D_{nm}^{(-)}\delta(t-t')(n,m = n_-, \varphi_-)$ are, respectively,

$$F_+ = \begin{pmatrix} 2\lambda n_0, & 4n_0\varepsilon\sin(\varphi_{20} + \varphi_{10}) \\ 0, & 2(\gamma + \lambda n_0) \end{pmatrix}, \qquad (43)$$

$$F_- = \begin{pmatrix} 2\gamma, & 4n_0\chi \sin n/\Delta \\ \Delta/n_0, & 0 \end{pmatrix}, \tag{44}$$

$$D^{(\pm)} = \pm \begin{pmatrix} 4n_0\gamma, & -2\varepsilon \sin (\varphi_{20}+\varphi_{10}) \\ -2\varepsilon \sin (\varphi_{20}+\varphi_{10}), & -\gamma/n_0 \end{pmatrix}. \tag{45}$$

Due to the decoupling between $(+)$ and $(-)$ combinations of the modes, we conclude that the following temporal correlation functions are equal to zero, $\langle \delta\varphi_+(t)\delta\varphi_-(t')\rangle = \langle \delta n_+(t)\delta n_-(t')\rangle = \langle \delta n_\pm(t)\delta\varphi_\mp(t')\rangle = 0$, and hence $\langle (\delta\varphi_1)^2\rangle = \langle (\delta\varphi_2)^2\rangle$, $\langle (\delta n_1)^2\rangle = \langle (\delta n_2)^2\rangle$. The other correlation functions can be calculated in the same way as described above for the below-threshold regime. The temporal correlation functions are derived as

$$\left\langle \begin{pmatrix} \delta n_\pm(t) \\ \delta\varphi_\pm(t) \end{pmatrix} (\delta n_\pm(t'), \delta\varphi_\pm(t')) \right\rangle = -\frac{1}{2} F_\pm^{-1} e^{-F_\pm^{-1}|t-t'|} D_\pm, \tag{46}$$

and hence

$$\left\langle \begin{pmatrix} \delta n_\pm \\ \delta\varphi_\pm \end{pmatrix} (\delta n_\pm, \delta\varphi_\pm) \right\rangle = -\frac{1}{2} F_\pm^{-1} D_\pm. \tag{47}$$

Performing the concrete calculations for each of the cases $\Delta > 0$ and $\Delta < 0$, we arrive at the following results:

$$\left\langle \begin{pmatrix} \delta n_+ \\ \delta\varphi_+ \end{pmatrix} (\delta n_+, \delta\varphi_+) \right\rangle = \frac{1}{4\lambda n_0(\gamma+\lambda n_0)} \begin{pmatrix} 4n_0[\gamma(\gamma+\lambda n_0)+(\chi-|\Delta|)^2], & -\lambda n_0(\chi-|\Delta|)\mathrm{sgn}(\Delta) \\ -2\lambda n_0(\chi-|\Delta|)\mathrm{sgn}(\Delta), & -\lambda\gamma \end{pmatrix}, \tag{48}$$

$$\left\langle \begin{pmatrix} \delta n_- \\ \delta\varphi_- \end{pmatrix} (\delta n_-, \delta\varphi_-) \right\rangle = \frac{1}{4|\Delta|\chi} \begin{pmatrix} 4n_0\chi(\chi-|\Delta|), & 2\chi\gamma \,\mathrm{sgn}(\Delta) \\ 2\chi\gamma \,\mathrm{sgn}(\Delta), & \frac{1}{n_0}[\gamma^2-|\Delta|(\chi-|\Delta|)] \end{pmatrix}. \tag{49}$$

We see that the considered system displays different types of quantum correlations in terms of the stochastic variables, namely between photon-number sum and phase sum in the modes, as well as between photon-number difference and phase difference in the modes. These results differ radically from the ones taking place for usual NOPO, where the correlation between photon-number difference and phase sum in the modes is realized. The results obtained indicate the possibilities to produce entanglement with respect to the new types of quantum correlations.

IV. CV ENTANGLEMENT IN THE PRESENCE OF PHASE-LOCKING

Let us now turn our attention to quantum-statistical effects and the entanglement production for the case of perfect symmetry between the modes $(\gamma_1=\gamma_2=\gamma, \Delta_1=\Delta_2=\Delta)$. Our aim in this section is to study the interplay between phase-locking phenomena and CV entanglement for the self-phase-locked NOPO. We note that unlike the two-mode squeezed vacuum state, the state generated in the above-threshold regime of NOPO is non-Gaussian, i.e., its Wigner function is non-Gaussian [17]. Recently, it has been demonstrated [18] that some systems involving beam splitters also generate non-Gaussian states. The general consideration of this problem for self-phase-locked NOPO seems to be very complicated. However, the mentioned results allow us to conclude that the state generated in self-phase-locked NOPO is most probably non-Gaussian. So far, the inseparability problem for a bipartite non-Gaussian state is far from being understood.

On the theoretical side, the necessary and sufficient conditions for the separability of bipartite CV systems have been fully developed only for Gaussian states, which are completely characterized by their first and second moments. To characterize the CV entanglement, we address both the inseparability and strong EPR entanglement criteria [19] which could be quantified by analyzing the variances of the relevant distance $V_-=V(X_1-X_2)$ and the total momentum $V_+=V(Y_1+Y_2)$ of the quadrature amplitudes of two modes $X_k=(1/\sqrt{2})[a_k^+\exp(-i\theta_k)+a_k\exp(i\theta_k)]$, $Y_k=(i/\sqrt{2})[a_k^+\exp(-i\theta_k)-a_k\exp(i\theta_k)]$ $(k=1,2)$, where $V(X)=\langle X^2\rangle-\langle X\rangle^2$ is a denotation for the variance and θ_k is the phase of local oscillator for the kth mode. The two quadratures X_k and Y_k are noncommuting observables. The inseparability criterion for the quantum state of two optical modes reads [19]

$$V = \frac{1}{2}(V_+ + V_-) < 1, \tag{50}$$

i.e., it indicates that the sum of variances drops below the level of vacuum fluctuations. Since the states of the system considered are non-Gaussian, the criterion (50) is only sufficient for inseparability. The strong EPR entanglement criterion is quantified by the product of variances as $V_+V_- < \frac{1}{4}$. We remind the reader that the sufficient condition for inseparability (50) in terms of the product of variances reads $V_+V_- < 1$, i.e., it is weaker than the strong EPR condition.

In order to obtain the general expressions for variances, we first write them in terms of the boson operators corresponding to the Hamiltonian (1). We perform the transformations $a_i \to a_i \exp(i\Phi_i)$, which restore the previous phase

structure of the intracavity interaction. Using also the symmetry relationships (4), we find quite generally the variances at some arbitrary quadrature phase angles θ_1, θ_2 as

$$V_{\pm} = V \pm R \cos(\Delta\theta), \qquad (51)$$

where

$$V = \frac{1}{2}(V_+ + V_-) = 1 + 2n - 2|\langle a_1 a_2 \rangle|\cos(\Sigma\theta + \Phi_{\text{arg}}), \quad (52)$$

$$R = 2\text{Re}(\langle a_1^2 \rangle e^{i\Sigma\theta}) - 2|\langle a_1^+ a_2 \rangle|, \qquad (53)$$

$$\Delta\theta = \theta_2 - \theta_1 - \Phi_\chi, \Sigma\theta = \theta_1 + \theta_2 + \Phi_l + \Phi_k, \qquad (54)$$

and $n = \langle a_1^+ a_1 \rangle = \langle a_2^+ a_2 \rangle$ is the mean photon number of the modes, $\Phi_{\text{arg}} = \arg\langle a_1 a_2 \rangle$. So, in accordance with the formula (51), the relative phase Φ_χ between the transformed modes gives the effect of the rotation of the quadrature amplitudes angle $\theta_2 - \theta_1$.

Obviously, the variances $V_{\pm}$ and hence the level of CV entanglement depend on all parameters of the system including the phases. The minimal possible level of V is realized for an appropriate selection of the phases θ_i, namely for $\theta_1 + \theta_2 = -\arg\langle a_1 a_2 \rangle - \Phi_l - \Phi_k$. Further, in most cases we assume that this phase relationship takes place, but we do not introduce new denotations for V and $V_{\pm}$ for the sake of simplicity. In this case ($\Sigma\theta = -\Phi_{\text{arg}}$), in correspondence with the formula (51), the variances $V_{\pm}$ depend only on the difference between phases $\Delta\theta$ and we arrive at

$$V = 1 + 2(n - |\langle a_1 a_2 \rangle|), \qquad (55)$$

$$R = 2\text{Re}(\langle a_1^2 \rangle e^{-i\Phi_{\text{arg}}}) - 2|\langle a_1^+ a_2 \rangle|. \qquad (56)$$

For the NOPO without additional polarization mixing, $\langle a_1^+ a_2 \rangle = \langle a_1^2 \rangle = \langle a_2^2 \rangle = 0$ and hence the case of the symmetric variances $V_+ = V_-$ is realized. The phase-locked NOPO generally has a nonsymmetric uncertainty region. However, the variances V_+ and V_- become equal for the special case of $\theta_2 - \theta_1 - \Phi_\chi = \pi/2$, when the inseparability condition reads $V < 1$ ($V = V_- = V_+$). We note that the relative phase Φ_χ plays an important role in specification of the entanglement.

A. Entanglement in the case of unitary time evolution

So far, we have considered mainly the steady-state regime of generation, including the effects of dissipation and cavity-induced feedback. However, in order to better understand the peculiarities of the entanglement for the system under consideration, it would be interesting and desirable to study the situation when the dissipation in the cavity is inessential and the evolution of the modes, due to their interactions, is described approximately by the master equation (2) without losses. In our analysis, we shall assume that both subharmonic modes are initially in the vacuum state. Then, the system's state in the absence of losses is generated from the vacuum state by the unitary transformation

$$|\Psi(t)\rangle = u(t)|0\rangle_1|0\rangle_2 = e^{-(i/\hbar)H_{\text{int}}t}|0\rangle_1|0\rangle_2, \qquad (57)$$

where

$$H_{\text{int}} = i\hbar\frac{kE}{\gamma_3}(a_1^+ a_2^+ - a_1 a_2) + \hbar\chi(a_1^+ a_2 + a_1 a_2^+). \qquad (58)$$

Here we neglect the pump depletion effects considering classically the amplitude of a driving field as a constant and we also consider the case of zero detunings $\Delta_1 = \Delta_2 = \Delta = 0$. For the cavity configuration considered, the validity of such an approximation is guaranteed for short interaction time intervals $(kE/\gamma_3)^{-1}, \chi^{-1} \lesssim \Delta t \ll \gamma^{-1}$, provided that the coupling constants kE/γ_3 and χ exceed the dumping rates of the modes.

Note that for $\chi \to 0$ the state (57) is transformed to the well-known two-mode squeezed state [20]. We note that while the entangled two-mode squeezed vacuum state is achieved in the laboratory (in the nondegenerate parametric amplifier [2]), the generation of the state (57) is an interesting option for the future. From an experimental point of view it can be realized in the combined scheme, that is, parametric down-conversion and wave plate, driven by a pulsed pump field. It is obvious that the interaction time Δt in this case is limited by the duration T of laser pulses, $\Delta t \lesssim T$. Roughly speaking, such a scheme is similar to the optical nondegenerate parametric amplifier in the presence of the phase-locking process, where the interaction time is increased by a cavity for both subharmonic modes. However, we note again that a complete study of the experimental configuration related to the nondissipative case is beyond the scope of this paper.

Now let us examine the entangled properties of the resultant state (57). Using formula (52), where $n = \langle u^{-1}(t)a_i^+ a_i u(t) \rangle$ and $\langle a_1(t)a_2(t) \rangle = \langle u^{-1}(t)a_1 a_2 u(t) \rangle$, after a long but straightforward algebra we get the final result for the variance $V = \frac{1}{2}(V_+ + V_-)$ for two different operational regimes: $\varepsilon < \chi$ and $\varepsilon > \chi$. The variance for the range $\varepsilon < \chi$ of a comparatively weak scaled pump field $\varepsilon = kE/\gamma_3$ reads

$$V(t) = 1 - \frac{\varepsilon^2}{\mu^2}[\cos(2\mu t) - 1] - \frac{\varepsilon}{\mu}\sin(2\mu t)\cos(\Sigma\theta), \quad (59)$$

where $\mu = \sqrt{\chi^2 - \varepsilon^2}$. Thus, we observe a periodic evolution of V in this regime typical for the linear coupling. The level of squeezing of the two modes is periodically repeated. The behavior of the two-mode variance also significantly depends on the phase-matching condition, so that we may tune the phase sum to maximize the entanglement. We further choose for illustrations the phase sum corresponding to $\cos(\Sigma\theta) = 1$ for both operational regimes. It seems perhaps more intuitive to study the time behavior scaled on the parameter $\varepsilon = kE/\gamma_3$, which contains the pump field amplitude and is an adjustable parameter of the system. The dependence of V versus the scaled time interval is shown in Fig. 2, where the three curves correspond to three different choices of the ratio ε/χ. Common to all curves is that the variance is nonclassical and squeezed at least at the points of its minima t_{min}, which can be obtained by the formula $ctg(2\mu t_{\text{min}}) = \varepsilon/\mu$. In all cases, the maximal degree of two-mode squeezing $V_{\text{min}} = V(t)|_{t=t_{\text{min}}} = 0.5$ is achieved in the limit $\varepsilon \to \chi$. For the curves in Fig. 2, the time intervals corresponding to the minimal values of V_{min} are equal to $\varepsilon t_{\text{min}} \simeq 0.14 + 0.20\pi k$
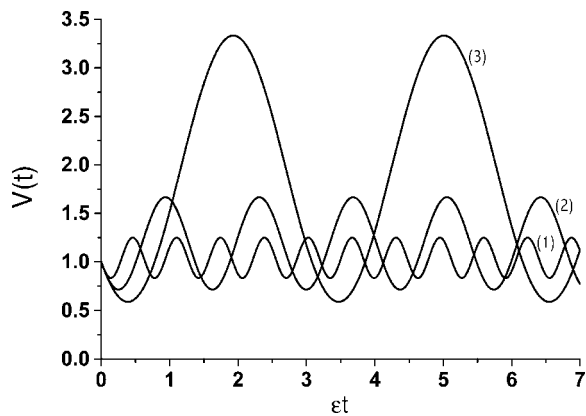
FIG. 2. Unitary evolution of the variance $V(t)$ versus the scaled dimensionless interaction time εt for the range of $\varepsilon < \chi$ and provided that $\cos(\Sigma \theta) = 1$. The parameters are $\varepsilon / \chi = 0.2$ (curve 1), $\varepsilon / \chi = 0.4$ (curve 2), and $\varepsilon / \chi = 0.7$ (curve 3).

(curve 1), $\varepsilon t_{min} \simeq 0.25 + 0.44 \pi k$ (curve 2), and $\varepsilon t_{min} \simeq 0.39 + 0.98 \pi k$ (curve 3) ($k = 0, 1, 2, \ldots$).

If the opposite inequality holds, $\varepsilon > \chi$, then the nonlinear parametric interaction becomes dominant over the linear coupling and the variance is given by the following formula:

$$V(t) = 1 + \frac{\varepsilon^2}{\eta^2}[\cosh(2\eta t) - 1] - \frac{\varepsilon}{\eta}\sinh(2\eta t)\cos(\Sigma \theta),$$

$$(60)$$

where $\eta = \sqrt{\varepsilon^2 - \chi^2}$.

For $\chi \to 0$ and $\cos(\Sigma \theta) = 1$, from this formula we arrive at a well-known result, $V(t) = \exp(-2\varepsilon t)$, for two-mode squeezed state. This shows that in the limit of infinite squeezing the corresponding state approaches a simultaneous eigenstate of $X_1 - X_2$ and $Y_1 + Y_2$, and thus becomes equivalent to the EPR state. Figure 3 shows the behavior of V when the system operates in the regime $\varepsilon > \chi$. This figure clearly shows that as the interaction time increases, the variance decreases and reaches its minimum. Then the squeeze variance exponentially increases with the growth of the interac-
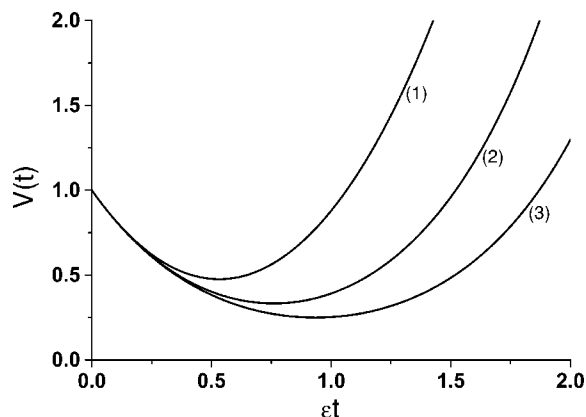
FIG. 3. Unitary time evolution of the variance $V(t)$ for the range of $\varepsilon > \chi$ and provided that $\cos(\Sigma \theta) = 1$. The parameters are $\varepsilon / \chi = 1.1$ (curve 1), $\varepsilon / \chi = 2$ (curve 2), and $\varepsilon / \chi = 3$ (curve 3).

tion time. For the data in Fig. 3 we obtain that the time intervals for which the variance reaches the minima are $\varepsilon t_{min} \simeq 0.53$ (curve 1), $\varepsilon t_{min} \simeq 0.76$ (curve 2), and $\varepsilon t_{min} \simeq 0.93$ (curve 3). It is easy to check that these points of minima can be found by the formula $ctgh(2\eta t_{min}) = \varepsilon / \eta$, provided that $\cos(\Sigma \theta) = 1$.

We also conclude that the variance squeezes up to a certain interaction time, if $\varepsilon > \chi$. It should be noted that although the time evolution of the variances is quite different for each of the operational regimes, the minimal values of the variance are described by the formula which is the same for both regimes,

$$V_{min} = V(t)_{t=t_{min}} = \frac{\chi}{\varepsilon + \chi}. \qquad (61)$$

With increasing ε / χ, in the regime $\varepsilon > \chi$, the minimal value of the variance decreases as $V_{min} \sim \chi / \varepsilon \ll 1$, which means that perfect squeezing takes place in the limit of an infinite pump field. This result is not at all trivial for the system considered, even in the absence of dissipation and cavity-induced feedback, because the insertion of a polarization mixer usually destroys the two-mode squeezing produced by nondegenerate parametric down-conversion. The reason is that the two-mode squeezed vacuum state is a superposition of two-photon Fock states $|n\rangle_1 |n\rangle_2$ and the polarization mixer destroys the Fock states having the same number of photons, i.e., $n_1 = n_2 = n$. The detailed analysis of this problem can be found, for example, in [14].

Having discussed the CV entanglement for nondissipative dynamics, we now turn our attention to the generation of entangled states of light beams in self-phase-locked NOPO, completely taking into consideration dissipation and cavity-induced feedback. The results will be presented in a steady-state regime of generation.

B. Entanglement in the self-phase-locked NOPO: Subthreshold regime

Using formulas (38) and (55), after some algebra, we obtain the minimal variance for the steady-state regime in the following form:

$$V = 1 + \frac{\varepsilon[\varepsilon S^2 - \sqrt{\gamma^2 S^4 + \Delta^2(S^2 - 2\chi^2)^2}]}{S^4 - 4\Delta^2\chi^2}. \qquad (62)$$

It is easy to check that in the limit $\chi \to 0$, the variance coincides with the analogous one for the ordinary NOPO, $V = V_- = V_+ = 1 - \varepsilon / (\varepsilon + \sqrt{\gamma^2 + \Delta^2})$. We see that the minimal variance remains less than unity for all values of pump intensity and is a monotonically decreasing function of ε^2. For all parameters, the maximal degree of two-mode squeezing $V \simeq 0,5$ is achieved within the threshold range. It is also easy to check that this expression is well-defined for all values of ε^2, including the vicinity of the threshold. One should keep in mind, however, that the linear approach used does not describe the threshold range where the level of quantum fluctuations increases. As a consequence, some matrix elements of Eqs. (38), (48), and (49) increase infinitely in the vicinity of threshold. Neverthe-
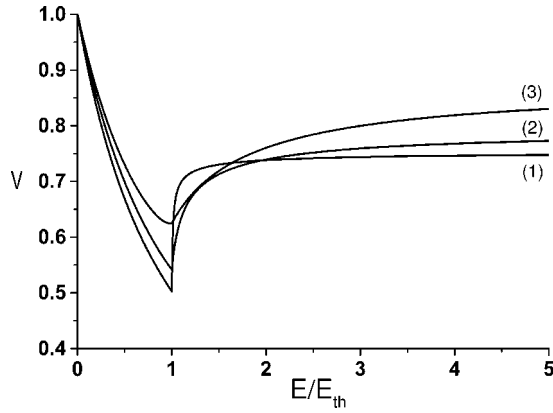
FIG. 4. The minimized variance V versus the dimensionless amplitude of the pump field $E/E_{th}=\varepsilon/\varepsilon_{th}$ for both operational regimes. ε_{th} and E_{th} are given by Eqs. (25) and (29). The parameters are $\chi/\gamma=0.1$ (weak coupling), $\Delta/\gamma=10$ (curve 1), $\chi/\gamma=0.5$ (moderate coupling), $\Delta/\gamma=3$ (curve 2), and $\chi/\gamma=0.5$, $\Delta/\gamma=1$ (curve 3).

less, it follows from Eq. (62) and further results (64)–(67) that such infinite terms are canceled in the variance V, as well as in V_-,V_+ for both operational regimes. This is not surprising, since such cancellation of infinities in the quadrature amplitude variances takes place for the ordinary NOPO also.

One of the differences between the squeezing effects of the ordinary and self-phase-locked NOPO is that the variances V_- and V_+ for the ordinary NOPO are equal to each other, while for the self-phase-locked NOPO they are in general different. The values of the nonsymmetric variances are expressed through R according to formula (51). This quantity can be calculated with the help of the formula (56). The result is found to be

$$R = \frac{\varepsilon\chi\Delta}{S^4 - 4\Delta^2\chi^2}\left[\frac{\varepsilon^4 - [\gamma^2 + (\Delta-\chi)^2][\gamma^2 + (\chi+\Delta)^2]}{\sqrt{\gamma^2 S^4 + \Delta^2(S^2 - 2\chi^2)^2}} + 2\varepsilon\right].$$

(63)

As we see, the final expressions (62) and (63) below the threshold are rather unwieldy. We show the corresponding numerical results in Figs. 4–6 for illustration.

C. Entanglement in the self-phase-locked NOPO: Above-threshold regime

Performing calculations for each of the cases $\Delta > 0$ and $\Delta < 0$, we find the variance V in the above-threshold regime in the following form:

$$V = \frac{3}{4} - \frac{1}{4\sqrt{1 + (\varepsilon_{th}/\gamma)^2[(\varepsilon/\varepsilon_{th})^2 - 1]}} + \frac{\chi}{4|\Delta|}.$$ (64)

To rewrite this expression through the original parameters, we should take into account that $E/E_{th}=\varepsilon/\varepsilon_{th}$ and $\varepsilon_{th}^2/\gamma^2 = (\chi/\gamma-|\Delta|/\gamma)^2+1$. The results (62) and (64) for both operational regimes are summarized in Fig. 4, where the variance V is plotted as a function of the amplitude of the pump field. One can immediately grasp from the figure that the sum of variances $V=\frac{1}{2}(V_+ + V_-)$ remains less than
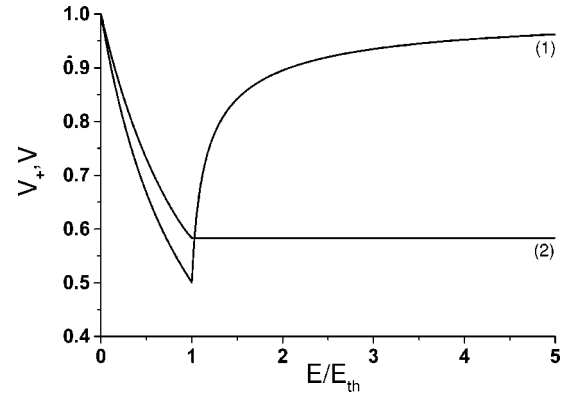
FIG. 5. The variances V_+ (curve 1) and V_- (curve 2) versus the dimensionless amplitude of the pump field $E/E_{th}=\varepsilon/\varepsilon_{th}$ for the parameters $\chi/\gamma=0.5$, $\Delta/\gamma=3$.

unity for all nonzero values of the pump field, provided that $\chi < |\Delta|$. This shows the nonseparability of the generated state. The maximal degree of entanglement is achieved in the vicinity of threshold, $V\simeq0,5$, if $\chi/|\Delta| \ll 1$. Far above the threshold, $E\gg E_{th}$, V increases with mean photon numbers of the modes and reaches the asymptotic value $V=3/4+\chi/4|\Delta|$. It should also be mentioned that the result (64) is expressed through the scaled pump-field amplitude $\varepsilon=kE/\gamma_3$ and hence depends on coupling constants k and χ.

We stress that the level of two-mode squeezing in the proposed scheme is limited due to the dissipation and pump depletion effects and reaches only 50% relative to the level of vacuum fluctuations if the pump intensity draws near to the generation threshold. Such limitation on the level of intracavity two-mode squeezing takes place also for the ordinary NOPO, as was been demonstrated in Refs. [12,22] by analysis of quantum fluctuations in the near-threshold range. Analogous conclusion has been made for one-mode squeezed light generated in OPO [23]. However, remember that these results pertain to the full squeezing of intracavity variances and not the spectra of the squeezing of output fields.
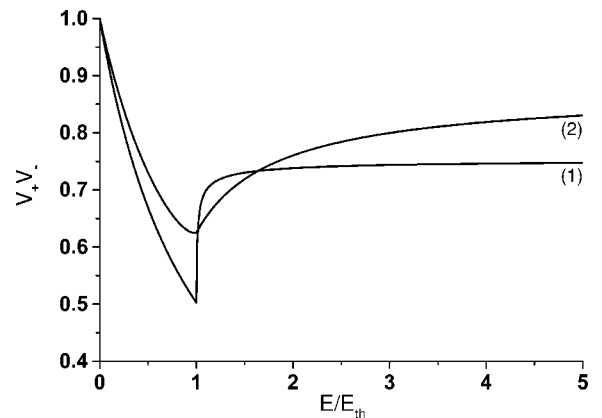
FIG. 6. The product of the variances V_+ and V_- versus the dimensionless amplitude of the pump field $E/E_{th}=\varepsilon/\varepsilon_{th}$ for the parameters $\chi/\gamma=0.1$, $\Delta/\gamma=10$ (curve 1) and $\chi/\gamma=0.5$, $\Delta/\gamma=1$ (curve 2).

As the last step in connecting two-mode squeezing to observables of CV entanglement, we report the expressions of the nonsymmetric variances calculated with the help of the formulas (51), (55), and (56). Upon evaluating all required expectation values, we obtain

$$R = \frac{\mathrm{sgn}(\Delta)}{4}\left(\frac{|\Delta| - \chi}{|\Delta|} - \frac{1}{\sqrt{1 + (\varepsilon^2 - \varepsilon_{th}^2)/\gamma^2}}\right) \quad (65)$$

and hence

$$V_+ = \frac{3|\Delta| + \chi + \mathrm{sgn}(\Delta)\cos(\Delta\theta)(|\Delta| - \chi)}{4|\Delta|}$$
$$- \frac{1 + \mathrm{sgn}(\Delta)\cos(\Delta\theta)}{4\sqrt{1 + (\varepsilon^2 - \varepsilon_{th}^2)/\gamma^2}}, \quad (66)$$

$$V_- = \frac{3|\Delta| + \chi - \mathrm{sgn}(\Delta)\cos(\Delta\theta)(|\Delta| - \chi)}{4|\Delta|}$$
$$- \frac{1 - \mathrm{sgn}(\Delta)\cos(\Delta\theta)}{4\sqrt{1 + (\varepsilon^2 - \varepsilon_{th}^2)/\gamma^2}}. \quad (67)$$

For the case of $\Delta\theta = 0$, when the variances are maximally different, the results are reduced to

$$V_- = \frac{1}{2} + \frac{\chi}{2\Delta},$$

$$V_+ = 1 - \frac{1}{2\sqrt{1 + (\varepsilon_{th}/\gamma)^2[(\varepsilon/\varepsilon_{th})^2 - 1]}} \quad (68)$$

for $\Delta < 0$. The case of $\Delta > 0$ is obtained from Eqs. (68) by exchanging $V_+ \to V_-$ and $V_- \to V_+$. These results for both operational regimes are depicted in Fig. 5. Some features are immediately evident. First of all, one can see that both variances are minimal in the critical range but show quite different dependences on the ratio $\varepsilon/\varepsilon_{th}$ above the threshold. An attentive reader may ask about the dependence of the results obtained on the parametric coupling constant k. We note in this connection that the squeezed variances are expressed through the scaled pump-field amplitude $\varepsilon = kE/\gamma_3$ and hence depend in general on both coupling constants k and χ.

In terms of demonstrating the CV strong EPR entanglement, one has to apply another criterion $V_+V_- < \frac{1}{4}$. For the case of the symmetric uncertainties ($V_+ = V_- = V$), the product of the variances $V^2 \geq \frac{1}{4}$ and hence the strong EPR entanglement cannot be realized. In the general case, the product of the variances reads

$$V_+V_- = V^2 - R^2\cos^2(\Delta\theta). \quad (69)$$

It seems that V_+V_- lies below $1/4$ at least for the relative phase $\Delta\theta = \pm\pi m$ ($m = 1, 2, \ldots$), and in the vicinity of threshold, where $V \simeq 0.5$. However, for such selection of the phases we arrive at

$$V_+V_- = \frac{|\Delta| + \chi}{4|\Delta|}\left(2 - \frac{1}{\sqrt{1 + (\varepsilon_{th}/\gamma)^2[(\varepsilon/\varepsilon_{th})^2 - 1]}}\right). \quad (70)$$

It is easy to check that the product of the variances exceeds $\frac{1}{4}$ even in the vicinity of the threshold. This quantity for both operational regimes is illustrated in Fig. 6. It should be noted again that a detailed analysis of this problem must include a more accurate consideration of quantum fluctuations in the critical ranges.

V. CONCLUSION

Our work demonstrates the possibility of the creation of CV entangled states of light beams in the presence of phase-localizing processes. We have called such quantum states the entangled self-phase-locked states of light [21] and we have shown that they can be generated in NOPO recently realized in experiment [6]. This device is based on the type II phase-matched down-conversion and additional phase-localizing mechanisms stipulated by the intracavity waveplate. The novelty is that this device provides a high level of phase coherence between the subharmonics, in contrast to what happens in the case of ordinary NOPO, where phase diffusion takes place. We have shown that both two-mode squeezing and quantum phase-locking phenomena are combined in such NOPO. This development paves the way towards the generation of bright CV entangled light beams with well-localized phases. It appears that this scheme involving phase locking may be useful for precise interferometric measurements and quantum communications, because it combines quantum entanglement and stability of type II phase matching with effective suppression of phase noise. Particularly, in practice, this phase-locked scheme can effectively be used in homodyne detection setups, as well as for observation of an interference with nonclassical light beams. We believe that such a source of bright entangled light providing phase coherence will also be applicable for realizing CV quantum teleportation. The price one has to pay for these advantages is the small aggravation of the degree of CV entanglement in a self-phase-locked NOPO in comparison with the case of an ordinary NOPO. The quantum theory of self-phase-locked NOPO has been developed in a linear treatment of quantum fluctuations for both below- and above-threshold regimes of generation. We have studied the CV entanglement as two-mode squeezing and have shown that entanglement is present in the entire range of pump intensities. In all cases the maximal degree of two-mode squeezing $V \simeq 0.5$ is achieved in the vicinity of the threshold, provided that the coupling constant χ is much less than the mode detunings. We have demonstrated that, as a rule, the highest degree of CV entanglement occurs for weak linear coupling strength χ. It has also been shown that the amount of entanglement can be controlled via the phase difference Φ_χ. The other peculiarities of the system of interest have been established for the case of unitary dynamics, which may be realized for the short interaction times in the case of pulsed pump fields. One of these concerns the presence of two operational regimes generating two-mode squeezing. If the linear coupling between subharmonics dominates over the parametric down-

conversion, $\varepsilon < \chi$, we have observed a periodic evolution of the squeezed variance. The maximal degree of squeezing has been $V \simeq 0,5$ in this regime. If the parametric interaction becomes dominant, $\varepsilon > \chi$, the higher degree of two-mode squeezing can be obtained, $V_{min} = [\chi/(\varepsilon + \chi)] < 0.5$, but up to a certain interaction time.

In our analysis, we have not investigated all possible quantum effects of self-phase-locked parametric dynamics. In particular, we have noted that the system considered displays different types of quantum correlations, but we have not analyzed their connection with all possible kinds of entanglement. This analysis might involve also the case of unitary dynamics, where the generalized two-mode squeezed state has been presented. Consideration of quantum fluctuations in the near-threshold operational range of self-phase-locked NOPO also deserves special attention for more accurate identification of CV entanglement. These topics are currently being explored and will be the subject of forthcoming work.

ACKNOWLEDGMENTS

[1] *Quantum Information Theory with Continuous Variables*, edited by S. L. Braunstein and A. K. Pati (Kluwer, Dordrecht, 2003), and references therein.

[2] S. L. Braunstein and H. J. Kimble, Phys. Rev. Lett. **80**, 869 (1998); A. Furusawa, J. L. Sorensen, S. L. Braunstein, C. A. Fuchs, H. J. Kimble, and E. S. Polzik, Science **282**, 706 (1998); W. P. Bowen, N. Treps, R. Schnabel, and P. K. Lam, Phys. Rev. Lett. **89**, 253601 (2002).

[3] J. Hald, J. L. Sorensen, C. Schori, and E. S. Polzik, Phys. Rev. Lett. **83**, 1319 (1999); B. Julsgaard, A. Kozhekin, and E. S. Polzik, Nature (London) **413**, 400 (2000); A. Kuzmich, L. Mandel, and N. P. Bigelow, Phys. Rev. Lett. **85**, 1594 (2000); L. M. Duan, J. I. Cirac, P. Zoller, and E. S. Polzik, *ibid.* **85**, 5643 (2000).

[4] M. D. Reid and P. D. Drummond, Phys. Rev. Lett. **60**, 2731 (1988); M. D. Reid, Phys. Rev. A **40**, 913 (1989); P. D. Drummond and M. D. Reid, *ibid.* **41**, 3930 (1990).

[5] Z. Y. Ou, S. F. Pereira, H. J. Kimble, and K. C. Peng, Phys. Rev. Lett. **68**, 3663 (1992); S. F. Pereira, Z. Y. Ou, and H. J. Kimble, Phys. Rev. A **62**, 042311 (2002).

[6] E. I. Mason and N. C. Wong, Opt. Lett. **23**, 1733 (1998).

[7] C. Fabre, E. I. Mason, and N. C. Wong, Opt. Commun. **170**, 299 (1999).

[8] G. Yu. Kryuchkyan and N. T. Muradyan, Phys. Lett. A **286**, 113 (2001); G. Yu. Kryuchkyan, L. A. Manukyan, and N. T. Muradyan, Opt. Commun. **190**, 245 (2001).

[9] J. J. Zondy, A. Douillet, A. Tallet, E. Ressayre, and M. L. Berre, Phys. Rev. A **63**, 023814 (2001).

[10] G. Yu. Kryuchkyan and K. V. Kheruntsyan, Zh. Eksp. Teor. Fiz. **103**, 18 (1993); **104**, 1161 (1994).

[11] Y. Zhang, H. Wang, X. Li, J. Jing, C. Xie, and K. Peng, Phys. Rev. A **62**, 023813 (2000); X. Li, Q. Pan, J. Jing, J. Zhang, C. Xie, and K. Peng, Phys. Rev. Lett. **88**, 047904 (2002).

[12] G. Yu. Kryuchkyan and L. A. Manukyan, Phys. Rev. A **69**, 013813 (2004).

[13] S. M. Tan, D. F. Walls, and M. J. Collett, Phys. Rev. Lett. **66**, 252 (1991); S. M. Tan, M. J. Holland, and D. F. Walls, Opt. Commun. **77**, 285 (1990); B. C. Sanders, K. S. Lee, and M. S. Kim, Phys. Rev. A **52**, 735 (1995); P. van Loock and S. L. Braunstein, Phys. Rev. Lett. **84**, 3482 (2000).

[14] M. S. Kim, W. Son, V. Buzek, and P. L. Knight, Phys. Rev. A **65**, 032323 (2002); X. B. Wang, *ibid.* **66**, 024303 (2002); **66**, 064304 (2002).

[15] P. D. Drummond and C. W. Gardiner, J. Phys. A **13**, 2353 (1980); K. J. McNeil and C. W. Gardiner, Phys. Rev. A **28**, 1560 (1983).

[16] M. D. Reid and P. D. Drummond, Phys. Rev. A **40**, 4493 (1989).

[17] K. V. Kheruntsyan and K. G. Petrosyan, Phys. Rev. A **62**, 015801 (2000).

[18] G. Toth, C. Simon, and J. I. Cirac, Phys. Rev. A **68**, 062310 (2003).

[19] L. M. Duan, G. Giedke, J. I. Cirac, and P. Zoller, Phys. Rev. Lett. **84**, 2722 (2000); R. Simon, *ibid.* **84**, 2726 (2000); G. Giedke, B. Kraus, M. Lewenstein, and J. I. Cirac, *ibid.* **87**, 167904 (2001); R. F. Werner and M. M. Wolf, *ibid.* **86**, 3658 (2001).

[20] B. Schumacher and C. M. Caves, Phys. Rev. A **31**, 3093 (1985).

[21] H. H. Adamyan and G. Yu. Kryuchkyan, e-print quant-ph/0309203.

[22] K. Dechoum, P. D. Drummond, S. Chaturvedi and M. D. Reid, e-print quant-ph/0310129.

[23] S. Chaturvedi, K. Dechoum, and P. D. Drummond, Phys. Rev. A **65**, 033805 (2002); P. D. Drummond, K. Dechoum, and S. Chaturvedi, *ibid.* **65**, 033806 (2002).